

## Auger Ejection of Electrons from Molybdenum by Noble Gas Ions

HOMER D. HAGSTRUM

*Bell Telephone Laboratories, Murray Hill, New Jersey*

(Received July 20, 1956)

Experimental investigation of electron ejection from atomically clean molybdenum by singly- and doubly-charged ions of the noble gases is reported. The basic measurements of electron yield and energy distribution of ejected electrons have been made for ions of kinetic energy in the range 10 to 1000 ev. Measurements are made at bombarding electron energies in the ion source below the threshold for formation of metastable ions. The electron ejection for molybdenum, as previously found for tungsten, has characteristics appropriate to ejection in Auger-type processes of neutralization and de-excitation at the metal surface. Values of 0.300, 0.254, 0.122, 0.069, and 0.022 were obtained for the electron yield for 10 ev He<sup>+</sup>, Ne<sup>+</sup>, Ar<sup>+</sup>, Kr<sup>+</sup>, and Xe<sup>+</sup> ions, respectively.

Extensive comparison of the present results with the work of others is possible. Comparison of the results for molybdenum and tungsten shows the differences to be largely attributable to the effect of work function change on the probability of escape of internally excited electrons from the metal. The Ne<sup>+</sup> ion shows the anomalies characteristic of the resonance neutralization and Auger de-excitation of a fraction of the ions at higher ion energies as was found for tungsten. Careful measurements have been made of yield and energy distributions of electrons ejected by doubly-charged ions. The processes by which a doubly-charged ion is de-excited and neutralized at a clean metal surface have been investigated in detail.

### I. INTRODUCTION

EXPERIMENTAL results of a study of electron ejection from atomically clean molybdenum by ions of the noble gases are presented in this paper. In a general way this work for molybdenum is similar to that already published for tungsten<sup>1,2</sup> but goes considerably beyond that previously published for molybdenum.<sup>3</sup> In the earlier work on molybdenum only helium ions were used; here studies are reported for the singly- and doubly-charged ions of all the noble gases. Although the results for tungsten and molybdenum are similar they differ significantly in a way which can be understood (Sec. VI) in terms of the theory already published.<sup>4</sup> Better data are available for molybdenum than for tungsten to show the onset of electron ejection by He<sup>+</sup> ions above 400-ev energy by a process which is not of the Auger type (Sec. III).

Electron ejection from molybdenum has been studied by many investigators in one way or another so that an extensive comparison of the present results with other work is possible (Sec. IV). Furthermore, ejection from molybdenum by metastable atoms has been studied by several investigators. Here a comparison (Sec. V) with the present results is particularly fruitful in view of the rather definite theoretical predictions concerning resonance transitions of electrons between the metal and the approaching atomic particle.

The electron yields and energy distributions of ejected electrons from doubly-charged ions have been carefully studied for molybdenum (Sec. VII). It is possible to reach rather definite conclusions concerning the processes in which doubly-charged ions and excited singly-charged ions are neutralized and de-excited at a clean metal surface.<sup>5</sup>

Experiment and apparatus are discussed very briefly in the next section inasmuch as the procedures are the same as previously used and reported.

### II. EXPERIMENT AND APPARATUS

The apparatus and experimental procedure used in this work are the same as were employed in the work on tungsten.<sup>1,2</sup> Detailed discussions are to be found in Secs. II and III of reference 1 and in a separate paper on experimental apparatus and procedure already published.<sup>6</sup> The instrument employed is the so-called Instrument II discussed in reference 6. In it ions formed by electron impact are mass analyzed and focussed by electrostatic lenses on the front surface of a ribbon target situated in the center of a spherical electron collector. The basic measurements are: (1) total electron yield with the electron collector 2 volts positive with respect to the target, and (2) energy distributions obtained by differentiating retarding potential data on electrons leaving the target. These measurements may be made at ion energies in the range 10 to 1000 ev.

Vacuum processing was carried out according to the "more drastic" procedure outlined in Sec. VII of reference 6. The target was cleaned by flashing to 2200°K and adsorption rate measurements for background gases in the instrument were made with the target itself. Liquid nitrogen was used on the traps when studying helium and neon. Then the background pressure was in the range  $1-4 \times 10^{-10}$  mm Hg and the monolayer adsorption time,  $\Delta t_m$ , was greater than 10 hours. When argon, krypton, and xenon were studied CO<sub>2</sub> and acetone were used on the traps. The background pressure then rose to the neighborhood of  $8 \times 10^{-9}$  mm Hg which is near the vapor pressure of Hg at 194.7°K. (See discussion in Sec. III of reference 1.) Total yield varied in the expected fashion with monolayer adsorption. All data reported here were recorded within one minute after starting to cool the target after a flash to 2200°K.

<sup>1</sup> H. D. Hagstrum, Phys. Rev. **96**, 325 (1954).

<sup>2</sup> H. D. Hagstrum, Phys. Rev. **103**, 317 (1956). Tungsten data of reference 1 corrected by removal of effects due to metastable ions of argon, krypton, and xenon.

<sup>3</sup> H. D. Hagstrum, Phys. Rev. **89**, 244 (1953).

<sup>4</sup> H. D. Hagstrum, Phys. Rev. **96**, 336 (1954).

<sup>5</sup> H. D. Hagstrum, Phys. Rev. **103**, 309 (1956).

<sup>6</sup> H. D. Hagstrum, Rev. Sci. Instr. **24**, 1122 (1953).

The target was then clean to within a few percent of a monolayer. Work function determinations from the slope of a Richardson plot (Sec. VIII of reference 6) gave  $\phi = 4.26, 4.38,$  and  $4.35$  ev on three occasions.

III. RESULTS FOR SINGLY-CHARGED IONS

In Fig. 1 are plotted the experimental data for total electron yield,  $\gamma_i$  as a function of the ion's incident kinetic energy in the range 10 to 1000 ev. These data were taken at bombarding electron energies in the ion source of 100, 100, 32, 28, and 22 ev for the He<sup>+</sup>, Ne<sup>+</sup>, A<sup>+</sup>, Kr<sup>+</sup>, and Xe<sup>+</sup> ions, respectively. In the last three cases these energies are just below the threshold for formation of metastable ions.<sup>5</sup> Metastable ions in helium are formed with such low probability as not to be detectable. There are no metastable levels of Ne<sup>+</sup>. Thus the data of Fig. 1 are free from effects of metastable ions and are to be compared with such data for tungsten recently published.<sup>2</sup> We observe that the general characteristics of the  $\gamma_i$  curves for molybdenum are the same as were found for tungsten.  $\gamma_i$  for He<sup>+</sup>

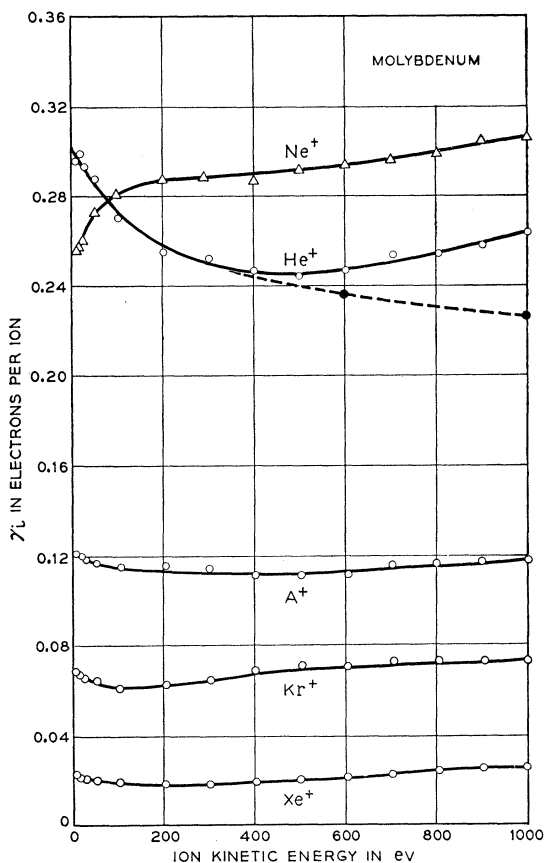


FIG. 1. Total electron yield,  $\gamma_i$ , versus ion kinetic energy for singly-charged ions of the noble gases incident on atomically clean molybdenum. The dashed curve lying below the experimental points for He<sup>+</sup> gives the variation of that part of  $\gamma_i$  which results from ejection in an Auger process. Determination of this curve is discussed in the text in connection with Fig. 5.

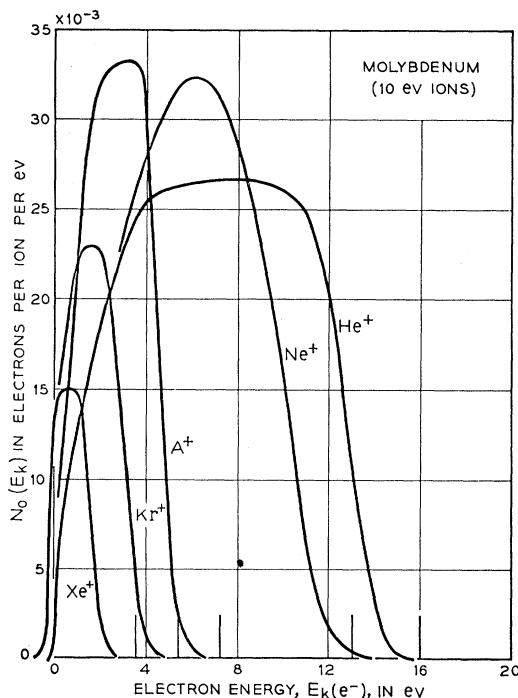


FIG. 2. Energy distributions of electrons ejected from atomically clean molybdenum by singly-charged ions of the noble gases of 10-ev incident kinetic energy. The vertical lines on the energy scale indicate the values of the quantity  $E_i - 2\phi$  listed in Table I.

initially falls, and then rises with ion energy above 400 ev.  $\gamma_i$  for Ne<sup>+</sup> rises rapidly at low ion energies and then more slowly. The  $\gamma_i$  curves for the heavier noble gases are quite constant except for a slight drop at low ion energies and a rise at higher energies.

The absolute values of the measured  $\gamma_i$  values for molybdenum are somewhat higher than those for tungsten (see Table I). This matter is discussed in detail in Sec. VI of this paper. The dashed curve lying below the experimental curve for He<sup>+</sup> at energies above 400 ev in Fig. 1 is discussed below in connection with Fig. 5.

In Figs. 2 and 3 are shown energy distribution functions for electrons ejected by singly-charged ions of 10- and 40-ev incident kinetic energy, respectively. These data were obtained from retarding potential curves by differentiation. The procedure followed here

TABLE I. Electron yields for 10-ev ions and values of  $E_i - 2\phi$ .

	$\gamma_i(\text{Mo})^a$	$\gamma_i(\text{W})^b$	$\gamma_i(\text{Mo})/\gamma_i(\text{W})$	$\gamma_{i2}(\text{Mo})^c$	$E_i - 2\phi^d$
He	0.300	0.290	1.04	0.81	16.04
Ne	0.254	0.213	1.19	0.68	13.02
A	0.122	0.095	1.29	0.42	7.22
Kr	0.069	0.050	1.38	0.39	5.46
Xe	0.022	0.013	1.69	0.30	3.59

<sup>a</sup> From Fig. 1 of this paper.

<sup>b</sup> From Fig. 1 of reference 2.

<sup>c</sup> From Fig. 11 of this paper.

<sup>d</sup> Ionization energy minus twice the work function of molybdenum.  $\phi(\text{Mo})$  is taken to be 4.27 ev.

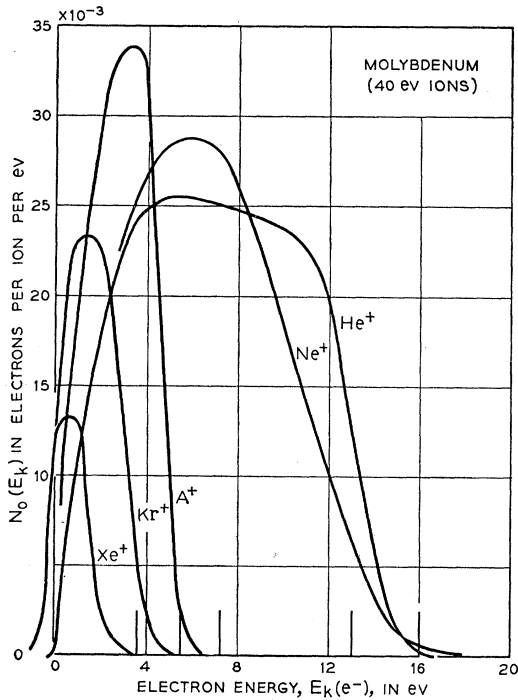


FIG. 3. Energy distributions like those of Fig. 2 except that the ion energy here is 40 ev. Note the violation of the kinetic energy limit  $E_i - 2\phi$  in the case of  $\text{Ne}^+$ .

was the same as used in the tungsten investigation (Sec. VI of reference 1). The basic data are target and collector currents,  $I_T$  and  $I_S$ , respectively, measured as functions of  $V_{ST}$ , the voltage between collector and target. For singly-charged ions the energy distribution  $N_0(E_k)$  is then equal to  $d\rho/dV_{ST}$ , where  $\rho = I_S/(I_T + I_S)$ . The electron energy scale is obtained from the  $V_{ST}$  scale by correcting for the measured contact potential (Sec. VIII of reference 6). A typical stepped curve of  $\Delta\rho/\Delta V_{ST}$  determined directly from the experimental data is shown in Fig. 4. Shown also in Fig. 4 are points for a smoothed  $d\rho/dV_{ST}$  curve which were calculated by a smoothing formula suggested by E. L. Kaplan. The formula, discussed in Sec. VI of reference 1, uses the data of 8 neighboring points weighted equally. The final  $N_0(E_k)$  curve as shown in Figs. 2 and 3 is a compromise between the smoothed curve and the  $\Delta\rho/\Delta V_{ST}$  stepped curve. This final curve follows the smoothed curve closely where  $d^2\rho/dV_{ST}^2$  is small but departs from it where the second derivative is high since the smoothing formula does not work well there. The reader is referred to a general discussion of the  $\rho(V_{ST})$  characteristic and its use in determining  $N_0(E_k)$  functions to be found in Sec. IX of reference 6. The fringing magnetic field from the analyzer magnet was compensated for in the target region by an auxiliary magnet which straddles the tube there.

The data of Figs. 2 and 3 were taken at the same bombarding electron energies in the source as specified

for Fig. 1 and are thus also for ions all of which are unexcited. Here again the data for molybdenum look similar to the corresponding data for tungsten. We note in particular that for all ions of 10-ev incident energy the maximum kinetic energy in each distribution agrees with the corresponding theoretical limit  $E_i - 2\phi$  (Fig. 2). We note also the violation in the case of neon at 40-ev ion energy in Fig. 3. Again this is interpreted to mean that all ions are neutralized in the process of Auger neutralization at 10 ev but that as energy increases, only in the case of  $\text{Ne}^+$  do some of the ions become excited atoms near the metal which are then de-excited in another Auger-type process. This latter process, called Auger de-excitation, can produce faster electrons and has a higher yield per ion than does Auger neutralization. Thus the violation of the  $E_i - 2\phi$  limit and the rise in  $\gamma_i(\text{Ne}^+)$  with ion energy are explained. These matters are discussed extensively in Sec. XI of the paper on theory.<sup>4</sup>

The initial drop in  $\gamma_i(\text{He}^+)$  with increasing ion energy to be seen in Figs. 2 and 3 is explained by the theory of Auger neutralization (Sec. XV of reference 4). It is the result of a reduction in effective ionization potential and increased broadening of the energy distribution as the  $\text{He}^+$  ion is Auger-neutralized on the average nearer to the metal surface as it approaches with greater velocity. The theory predicts a steady drop in  $\gamma_i(\text{He}^+)$  and cannot account for the experimentally observed rise above

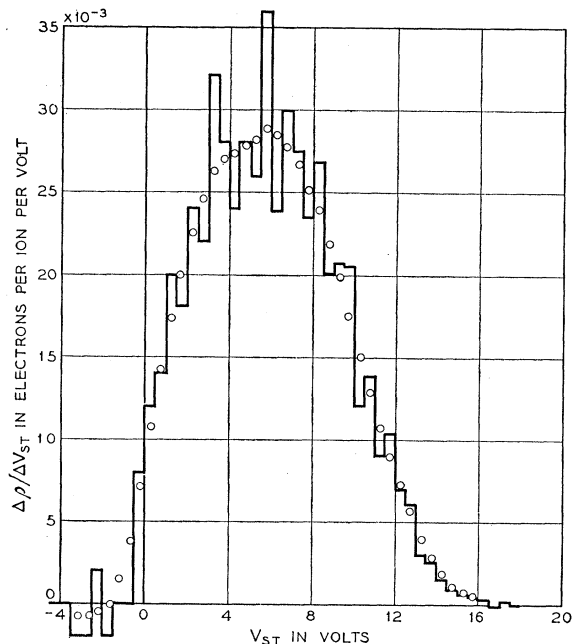


FIG. 4. Typical data from which the energy distribution function  $N_0(E_k)$  is obtained. The stepped curve is the derivative curve  $\Delta\rho/\Delta V_{ST}$  obtained directly from the experimental data. The points are smoothed values of  $d\rho/dV_{ST}$  obtained from a formula which makes use of eight adjacent data points. These curves are for  $\text{Ne}^+$  ions of 40-ev energy and may be compared with the curve for  $\text{Ne}^+$  in Fig. 3. See further discussion in Sec. III of the text.

400 ev. This rise has been attributed to the ejection of electrons in a process other than an Auger process setting in above 400 ev. This idea is strongly supported by the behavior of the energy distribution function as ion energy is increased. Here better data are available for molybdenum than tungsten.

In Fig. 5,  $N_0(E_k)$  functions are plotted for  $\text{He}^+$  ions of 10, 40, 100, 200, 600, and 1000 ev initial energy. The first four of these curves are for energies which lie on the falling part of the  $\gamma_i$  characteristic. They vary systematically in a way accountable for by theory. The maximum reduces and the high-energy tail extends with increasing ion energy as predicted by energy level shifts near the metal and the effects of the Heisenberg uncertainty principle. The  $N_0$  curves at 600 and 1000 ev, on the other hand, lie at energies on the rising part of the  $\gamma_i(\text{He}^+)$  curve and differ in a significant manner from the other four curves. We note in Fig. 5 the appearance of additional electrons at low energies which account for the rise in  $\gamma_i$ . These electrons cannot arise in the process of Auger neutralization for then they would be distributed over that part of the distribution which does arise from the Auger process. The bump on the right-hand side of each of these curves suggests that the curves are compounded of two. The dashed line suggests the form to be expected for the Auger part. If this is the true state of affairs, the Auger part would vary with energy as expected. The area under the dashed curve should then give the  $\gamma_i$  values attributable to the Auger process only. These values for 600 and

1000 ev are plotted as the full circles of Fig. 1 and are seen to lie on a smooth extension (dashed line) of the falling  $\gamma_i$  characteristic. Such behavior is quantitatively in agreement with theory. In Table XIII of reference 4 calculated  $\gamma_i$  values (there called  $\gamma_N$ ) show such a steady drop with increasing ion energy. It is thought that each ion undergoes Auger neutralization at all energies but that at the higher energies the neutralized particle is capable of releasing additional electrons on closer approach to the metal lattice. We note that  $\text{He}^+$ , being the lightest of the noble gas ions, moves the fastest for a given energy. The electrons ejected in the non-Auger process, like those observed for contaminated metal surfaces,<sup>7</sup> are slower than those ejected in the Auger process.

We may now compare the results presented here with those previously published for the helium ions only.<sup>8</sup> In general the results agree quite well. What differences there are attributable to better target surface conditions and to better means of extracting the  $N_0(E_k)$  functions from the original data in the present work.

The older  $\gamma_i$  data (Fig. 6 of reference 3) lie somewhat lower than those of Fig. 1. At 10 ev,  $\gamma_i$  was earlier reported at 0.25 against the present value of 0.30. This is perhaps the result of a cleaner target in the present work. The  $\gamma_i$  value is extremely sensitive to even a small fraction of a monolayer on the target surface. Other work<sup>7</sup> indicates that one monolayer will drop  $\gamma_i(\text{He}^+)$  at 10 ev for tungsten from 0.29 to 0.18.  $\gamma_i$  has dropped to 0.25 at a coverage between 10 and 15% of a monolayer. Thus only a slightly contaminated surface in the earlier work could account for the reduced  $\gamma_i$ . In the present work the target was flashed hotter (2200°K vs 1750°K) and considerably better background pressures were attained. The small differences between the older and present  $N_0(E_k)$  results are attributable to improved reduction of the data. In the older work the  $N_0(E_k)$  function was determined graphically as the slope of the  $\rho(V_{ST})$  curve.

#### IV. COMPARISON OF $\gamma_i$ WITH THE RESULTS OF OTHERS

Electron ejection from molybdenum has been investigated repeatedly. It is the purpose here, however, to discuss in detail only those results which were obtained under conditions reasonably comparable to those of the present work.

Varney<sup>8</sup> has published the most recent measurements of yield from molybdenum. He determined  $\gamma_i$  by a method involving the determination of a particular form of current transient during a pulsed Townsend discharge. The conditions of voltage, gas pressure, and plate separation yielding the desired form made it possible to calculate  $\gamma_i$ . The quantity  $\gamma_i$  was obtained as a function of  $E/p_0$  and found first to increase with

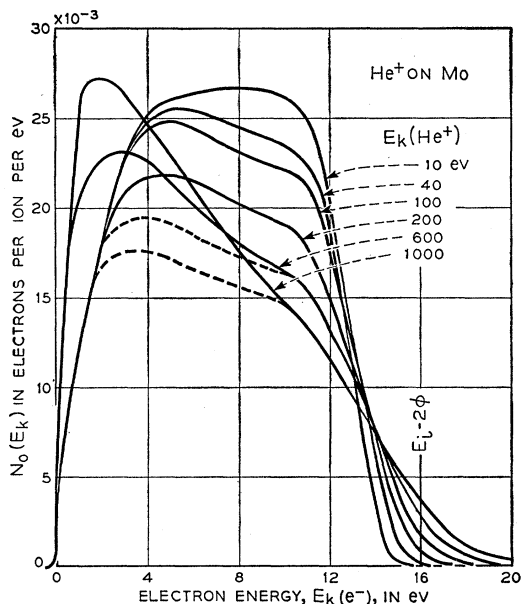


FIG. 5. Energy distribution functions of electrons ejected from molybdenum by  $\text{He}^+$  ions of various incident kinetic energies. Note the smooth variation from curve to curve for  $E_k(\text{He}^+) < 400$  ev and the appearance of a peak near zero electron energy for  $E_k(\text{He}^+) > 400$  ev. The dashed lines separate the distributions at 600- and 1000-ev ion energy into parts attributable to Auger and non-Auger processes of electron ejection.

<sup>7</sup> H. D. Hagstrum (to be published).

<sup>8</sup> R. N. Varney, Phys. Rev. **93**, 1156 (1954).

TABLE II.  $\gamma_i$  data for singly-charged noble gas ions on molybdenum obtained under conditions considered at all comparable with the present work.

	Varney <sup>a</sup>	Molnar <sup>b</sup>	Lauer <sup>c</sup>	Depp <sup>d</sup>	Present work <sup>e</sup>
Ne <sup>+</sup>	0.20			0.228	0.254
A <sup>+</sup>	0.083	0.071	0.035– 0.051	0.112	0.122
Kr <sup>+</sup>	0.053				0.069

<sup>a</sup> Reference 8.

<sup>b</sup> Reference 9.

<sup>c</sup> These are Lauer's data (reference 12) as corrected by Theobald (reference 11) for electron back-scattering.

<sup>d</sup> These are values of  $\gamma_i$  calculated from Depp's breakdown voltages (reference 13) using the ionization coefficient data of Kruithof (reference 14). See text and Table III.

<sup>e</sup> For 10-ev ions from Table I.

increasing  $E/p_0$  and then to level off at a constant value. This behavior was attributed to back reflection of electrons by the gas atoms at the lower  $E/p_0$ . At higher  $E/p_0$ , the values  $\gamma_i=0.20$ , 0.083, and 0.053 were obtained for Ne<sup>+</sup>, A<sup>+</sup>, and Kr<sup>+</sup>, respectively. These values are listed in Table II along with the results of other work considered reasonably comparable to the present work. Varney compared his work with the present author's preliminary measurements on tungsten but a direct comparison for molybdenum is now possible. Before discussing these results, those of other authors will be presented.

Molnar has determined electron yields for ions,  $\gamma_i$ , and metastable atoms,  $\gamma_m$ , from measurements<sup>9</sup> of transient currents in a pulsed Townsend discharge using his theory<sup>10</sup> of the phenomenon. His value of  $\gamma_i$  for A<sup>+</sup> at the highest value of  $E/p_0$  he used is also listed in Table II.

Theobald,<sup>11</sup> in an investigation of back diffusion of photoelectrons to a cathode in a gas, has applied his measured corrections for the effect to the results which Lauer<sup>12</sup> measured for  $\gamma$  in some studies of the pulsed positive wire corona at high pressure and low  $E/p_0$  at the cathode cylinder. These results are also shown in Table II. Finally, it has been possible to calculate values for  $\gamma_i$  for Ne<sup>+</sup> and A<sup>+</sup> on molybdenum from careful breakdown voltage measurements made by Depp.<sup>13</sup> Depp reports measured breakdown voltages,  $V_B$ , at various values of  $p_0d$  and gives the corresponding value of  $E/p_0$ . These data are used along with Kruithof's values<sup>14</sup> of  $\eta$  and  $V_0$  to calculate  $\gamma$  from the expression  $\gamma=1/[\exp\eta(V_B-V_0)-1]$ . Numbers pertinent to the calculation are listed in Table III. These calculated  $\gamma$  values include the effects of back diffusion of electrons as well as possible contributions to  $\gamma$  from radiation and metastable atoms as well as ions. Molnar<sup>9</sup> finds

<sup>9</sup> J. P. Molnar, Phys. Rev. **83**, 940 (1951).

<sup>10</sup> J. P. Molnar, Phys. Rev. **83**, 933 (1951).

<sup>11</sup> J. K. Theobald, J. Appl. Phys. **24**, 123 (1953).

<sup>12</sup> E. J. Lauer, J. Appl. Phys. **23**, 300 (1952).

<sup>13</sup> W. A. Depp (private communication of results obtained in the gas tube development group of Bell Laboratories in the course of development of voltage reference tubes).

<sup>14</sup> A. A. Kruithof, Physica **7**, 519 (1940).

that, at the higher  $E/p_0$  in the range of Depp's measurements, the escape probability into the gas of an electron emitted from the cathode is 97%. The other effects are discussed below.

Of the data presented in Table II, it is this writer's opinion that those of Depp and the present work are the most comparable. It would appear that both relate to atomically clean surfaces. The breakdown voltage data were taken under carefully controlled conditions with molybdenum metal sputtered all over the interior of the tube. Since the  $\gamma$  from breakdown data corresponds to a much slower ion than 10 ev, we see a possible reason for the greater discrepancy in the case of Ne<sup>+</sup> than A<sup>+</sup>. We note in Fig. 1 that  $\gamma_i(\text{Ne}^+)$  is a much more rapidly varying function of ion energy at low energies than is  $\gamma_i(\text{A}^+)$ . It is interesting to note that the ratio of the values of  $\gamma$  for A<sup>+</sup>, 0.112/0.122, is 0.92 which, in the light of Molnar's results, is not an unreasonable back reflection factor. Any presence of radiative or metastable effects in the breakdown measurements must reduce the true  $\gamma_i$  below the  $\gamma$  value specified. The good agreement with the present results, however, makes one suspect that these effects are small.

It is the author's opinion that the data of Varney, Molnar, and Lauer represent results for cathode surfaces which are covered with the order of a monolayer of foreign gas. The  $\gamma_i$  values are in the proper range for surfaces covered with a monolayer. Witness the drop in  $\gamma_i$  at low energies for He<sup>+</sup> on Mo as the surface is covered as shown in Fig. 6 of reference 3. It is also difficult to see how the cathode could be maintained atomically clean over many hours under the conditions of the experiments as described.

Many other measurements of  $\gamma_i$  for molybdenum surfaces are to be found in the literature. All are for apparently heavily contaminated surfaces or are questionable on other grounds. Perhaps the most quoted work is that of Oliphant.<sup>15</sup> Oliphant presents  $\gamma_i$  data which, because the  $\gamma_i$  is so low, appear to refer to a contaminated surface even for a hot target. He obtains energy distributions both by retarding potentials and by magnetic analysis which extend beyond the energies observed in the present work and indicate structure not now found. Since this structure is observed by both methods of velocity analysis, it is undoubtedly true that

TABLE III. Numbers pertinent to the calculation of  $\gamma$  from the breakdown voltage at the Paschen minimum.

	$V_B^a$ volts	$p_0^a$ mm Hg	$E/p_0^a$ volts/ cm mm	$V_0^b$ volts	$\eta^b$ ions/ volt	$\gamma$ elec- trons/ ion
Ne	143	100	80	30	0.0149	0.228
A	121	25	200	17	0.0221	0.112

<sup>a</sup> W. A. Depp, reference 13.

<sup>b</sup> A. A. Kruithof, reference 14.

<sup>15</sup> M. L. E. Oliphant, Proc. Roy. Soc. (London) **A127**, 373 (1930).

the electrons analyzed had these velocities. It is the present writer's opinion, however, that these effects are not characteristic of the electron ejection phenomenon but of some aspect of the experimental arrangement. Oliphant's ion beam was not mass-analyzed, for example, and undoubtedly contained both singly- and doubly-charged ions in proportions which could be functions of the ion beam energy. In another publication<sup>16</sup> Oliphant presents data for helium metastable atoms on a molybdenum surface. In the next section we shall discuss the fact that one would expect the  $N_0(E_k)$  function for this to be the same as that for ions. It is thus significant that Oliphant's metastable experiments are explainable in terms of later work but his ion experiments are not. This is thought again to point to a problem connected with the ion beam rather than the means of analyzing the ejected electrons.

#### V. COMPARISON WITH EXPERIMENTS EMPLOYING METASTABLE ATOMS

Two experiments reported in the literature employ beams of metastable atoms incident on a molybdenum surface. These are the work of Oliphant<sup>16</sup> and of Greene.<sup>17</sup> Since the results of these investigators are quite similar, only those of Greene will be considered

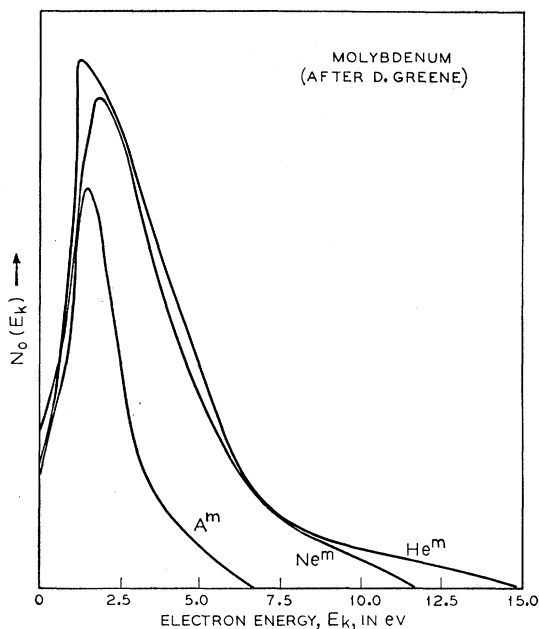


FIG. 6. Energy distributions measured by Greene (reference 17) for metastable atoms of He, Ne, and A incident on a molybdenum surface which was undoubtedly covered with a least a monolayer of foreign gas. These curves look like what is observed for ions and cannot be explained in terms of Auger de-excitation of the metastables. As explained in the text, this is strong evidence supporting the view that the metastables are in fact ionized at the metal before they undergo any Auger process.

<sup>16</sup> M. L. E. Oliphant, Proc. Roy. Soc. (London) **A124**, 228 (1929).

<sup>17</sup> D. Greene, Proc. Phys. Soc. (London) **B63**, 876 (1950).

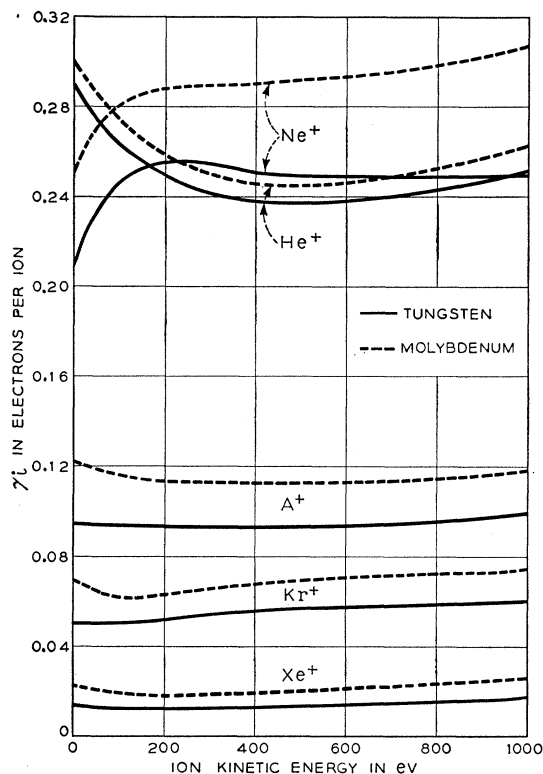


FIG. 7. Comparison of  $\gamma_i$  data for atomically clean tungsten and molybdenum. The ratios of  $\gamma_i$  values for 10-eV ions are listed in Table I.

here. Energy distributions observed by Greene for metastable atoms of helium, neon, and argon are reproduced in Fig. 6. Greene calculated a maximum energy by the relation  $E_x - \phi$ , the excitation energy minus the work function of the metal. He also calculated a minimum energy  $E_x - \epsilon_0$ , the excitation energy minus the barrier height in the metal. Although he used much too large a value of  $\epsilon_0$  (17.9 eV instead of something near 10.9 eV), he calculated a definite minimum energy of 1.9 eV for helium and attempted to explain why he did not observe it. If we use a value of  $\epsilon_0 = 10.9$  eV equal to Manning and Chodrow's calculated value for tungsten<sup>18</sup> (see Sec. VI), we calculate a minimum energy of  $19.8 - 10.9 = 8.9$  eV for the electrons ejected by helium metastable atoms. This is clearly far from what either Oliphant or Greene observed. None of the reasons Greene has listed appear capable of accounting for the discrepancy, nor should the geometry of the target and electron collector be capable of producing so startling an effect.

Varnerin<sup>19</sup> and the author<sup>20</sup> independently have realized that because of the relative ease with which

<sup>18</sup> M. F. Manning and M. J. Chodorow, Phys. Rev. **56**, 787 (1939).

<sup>19</sup> L. J. Varnerin, Jr., Phys. Rev. **91**, 859 (1953).

<sup>20</sup> H. D. Hagstrum, Phys. Rev. **91**, 543 (1953), Sec. V. See also reference 4, Sec. XI.

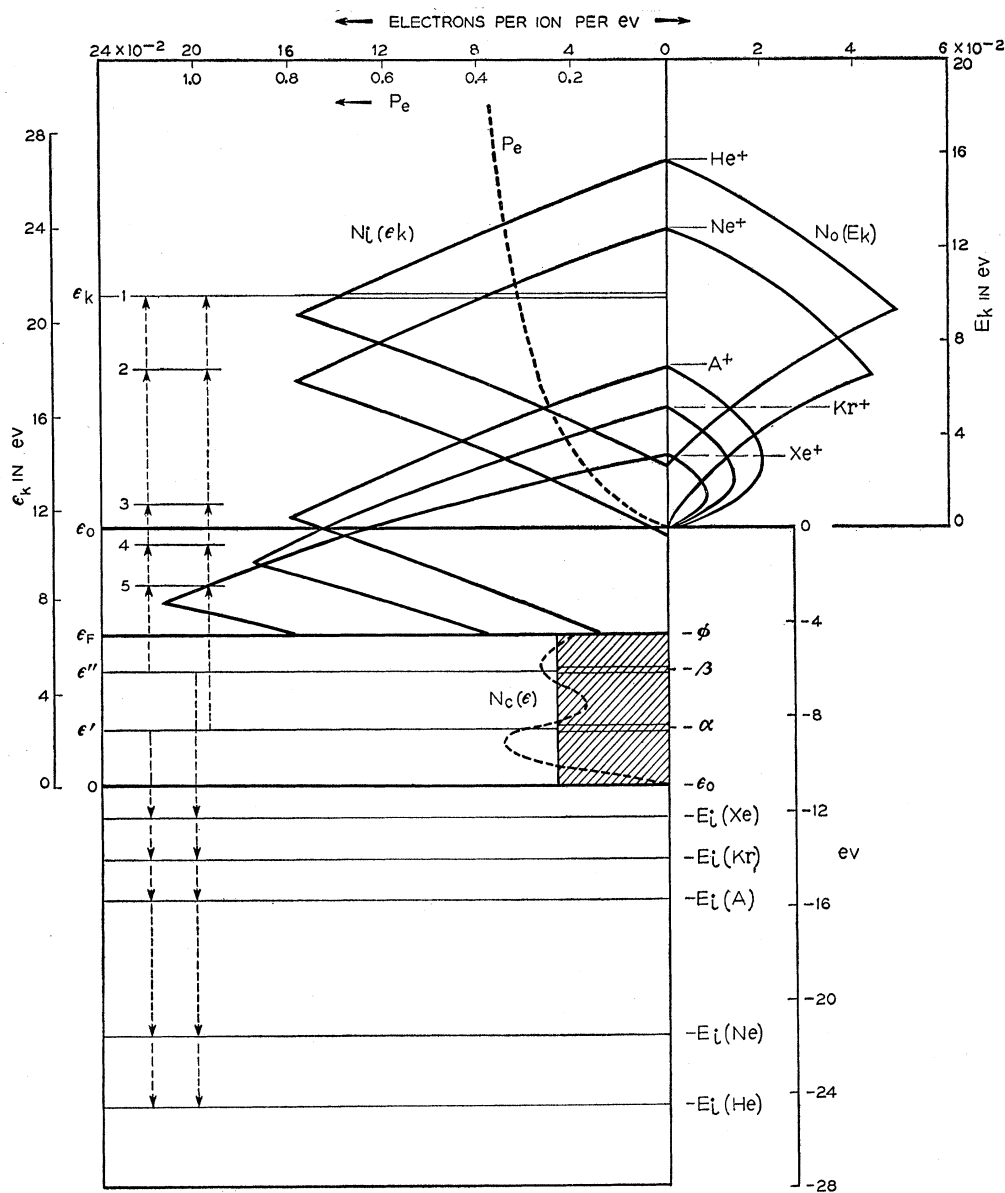


FIG. 8. Energy level diagram illustrating the essentials of the process of Auger neutralization of singly-charged ions of the noble gases at the surface of a metal like tungsten or molybdenum. The horizontal line  $0-0(\epsilon_k = \epsilon_0, E_k = 0)$  is the vacuum level (energy of an electron at rest at an infinite distance from the metal).  $N_c(\epsilon)$  is the state density function plotted to the left.  $N_c(\epsilon) = \text{constant}$  and the  $N_c(\epsilon)$  function calculated by Manning and Chodorow (reference 18) are shown. Electronic transitions characteristic of the Auger neutralization process are shown at the left.  $N_i(\epsilon_k)$  is the distribution in energy of internally excited electrons shown for each ion. Its maximum kinetic energy lies at  $\epsilon_k = E_i + \epsilon_F - \phi$ ,  $E_k = E_i - 2\phi$ .  $P_e$  is the probability of escape of internally excited electrons from the metal and  $N_0(E_k)$  is the distribution in energy of electrons which leave the metal.  $\gamma_i$  is the area under the  $N_0(E_k)$  function.

electrons tunnel between the metal and an arriving atomic particle, the nature of the particle at the time it becomes involved in an Auger process does not depend on its nature at large distances from the metal. The positions of energy levels in atom and metal make it highly probable that a helium metastable will be ionized on approaching a metal like molybdenum and that it will subsequently be neutralized in the process of Auger

neutralization. Thus what Greene and Oliphant observed were electrons ejected by the singly-charged ion even though they sent metastable atoms toward the surface. In fact, Greene's data of Fig. 6 look much like what one would expect for the singly-charged ion incident on a somewhat contaminated surface. It has been found<sup>7</sup> that contamination of the surface decreases the relative number of faster electrons observed. The

kinetic energy maxima of Greene's curves are in reasonable agreement with the  $E_i - 2\phi$  values of Table I. One would expect them to be lower because his surface most likely had a larger work function than an atomically clean surface. Furthermore, kinetic energy minima to be expected are zero for Ne and A and 2.8 eV for He, if one uses the  $\epsilon_0$  for an atomically clean surface. A contaminated surface would give a lower minimum. Furthermore, the minimum of 2.8 eV is calculated neglecting energy level shifts and the broadening by virtue of the Heisenberg principle. All of these effects plus the geometrical one would certainly make the minimum energy unobservable in agreement with Greene's and the present experiments.

The above ideas concerning the resonance ionization of a metastable atom near a metal before any Auger process occurs would mean that for slow ions  $\gamma_m \equiv \gamma_i$ . This is in fact what was found to be the case within experimental error by Molnar.<sup>9</sup>

VI. SIGNIFICANCE OF DIFFERENCES BETWEEN RESULTS FOR MOLYBDENUM AND TUNGSTEN

We have noted earlier that although the results for molybdenum and tungsten are similar, there exist significant differences between them. For convenience the  $\gamma_i$  data for Mo and W are plotted on the same graph in Fig. 7. We note that  $\gamma_i$  is greater for Mo than for W and the more so the lower the ionization energy

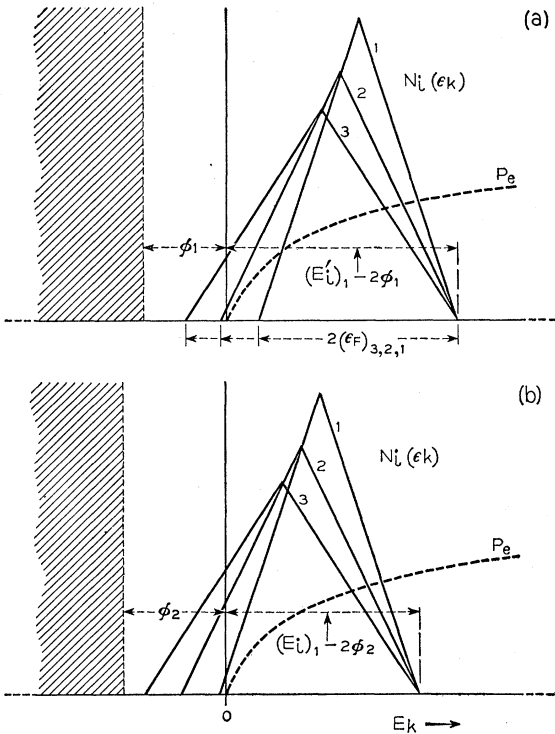


FIG. 9.  $N_i(\epsilon_k)$  distribution functions for two different work functions  $\phi$ , parts (a) and (b), and in each part for three different widths of the filled band,  $\epsilon_F$ . These are for a distribution which lies almost entirely above the vacuum level,  $E_k=0$ .

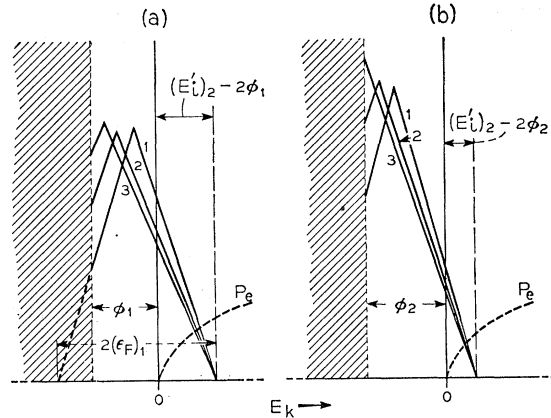


FIG. 10.  $N_i(\epsilon_k)$  distribution functions like those of Fig. 9, but for the case in which only the high-energy tail of the distribution lies at energies above the vacuum level.

of the atom. Thus, as is listed in Table I, the ratio  $\gamma_i(\text{Mo})/\gamma_i(\text{W})$  for 10-eV ions ranges from 1.04 for He to 1.69 for Xe. We inquire now into the theoretical reasons for these differences. The considerations of this section presuppose some familiarity with the theoretical ideas concerning Auger processes near metal surfaces already published.<sup>4</sup>

In the energy level diagram of Fig. 8 are to be seen the essential features of electron ejection by the process of Auger neutralization. For simplicity we have assumed a constant density of states in the conduction band (Manning and Chodorow's calculated density function for tungsten<sup>18</sup> is also shown) and have neglected the effects of energy level shifts near the metal and the Heisenberg uncertainty principle. Thus the energy distributions of internally excited electrons are approximate triangles. The probability of escape function,  $P_e$ , used is that previously obtained<sup>4</sup> by fitting the theory to the data for  $\text{He}^+$  on W.

We now ask our question again. What differences could there be between tungsten and molybdenum which could result in different  $\gamma_i$  values with those for molybdenum coming out to be the higher?

There are three changes in metal characteristics which would lead to an increase in  $\gamma_i$  for each of the noble gas ions. These are:

1. A decrease in work function  $\phi$ . Since the maximum kinetic energy for both the  $N_i$  and  $N_0$  distribution lies at  $E_i - 2\phi$  and the width of the  $N_i$  function at its base is  $2\epsilon_F$ , independent of  $\phi$ , we see that a decrease in  $\phi$  will shift the  $N_i$  function to higher energies and thus higher escape probabilities resulting in a larger  $\gamma_i$ .

2. A decrease in  $\epsilon_F$ , the width of the filled band in the metal. This would result in a decrease in the base width of the  $N_i$  function leaving the position of its maximum kinetic energy the same. This would lead to an increase in  $\gamma_i$  because more electrons would have greater energies.

3. A variation of the state density function putting



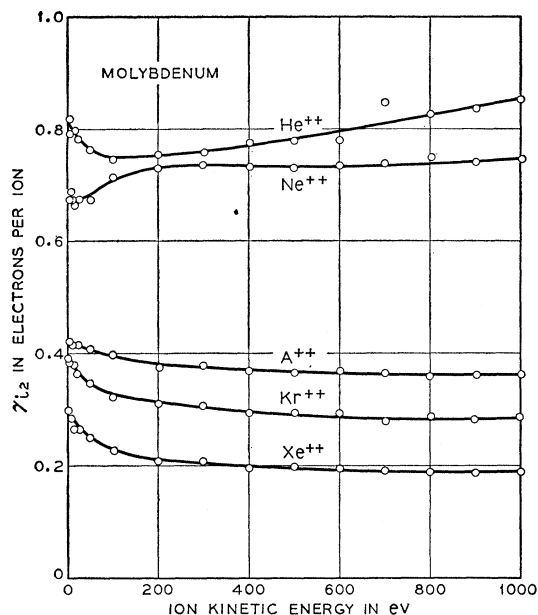


FIG. 11. Electron yield,  $\gamma_{i2}$ , for doubly-charged ions of the noble gases incident on atomically clean molybdenum.

more electrons higher in the filled band. Since this results in  $N_i$  functions which are greater in magnitude nearer their higher energy limits,  $\gamma_i$  increases.

The effects on the  $N_i$  function of changes in  $\varphi$  and  $\epsilon_F$  (items 1 and 2 above) are shown in Figs. 9 and 10. Figure 9 shows  $N_i$  functions which lie almost entirely above the vacuum level,  $\epsilon_k > \epsilon_0$ ,  $E_k > 0$ , as is the case for He<sup>+</sup>. Figure 10 shows the situation for an  $N_i$  function of which only the high-energy tail lies above the vacuum level as for Xe<sup>+</sup>. In each of the figures two values of work function are chosen, parts (a) and (b), and within each of these parts three values of  $\epsilon_F$  are shown. We may judge the effect on  $\gamma_i$  of these changes by imagining each  $N_i$  function to be multiplied by the probability of escape  $P_e$  to obtain the  $N_0$  function and estimating the change in its area. It is perhaps evident from Fig. 9 that the change of either  $\epsilon_F$  or  $\varphi$  will change  $\gamma_i$  but not by amounts that are very different. This is not the case, however, for the situation depicted in Fig. 10. Here it is evident that for either value of  $\varphi$  a change in  $\epsilon_F$  will alter  $\gamma_i$  little but a change in  $\varphi$  itself, since it changes the length of tail projecting above the vacuum level, will change  $\gamma_i$  by a much larger amount.

Inasmuch as the experiment shows a large change in  $\gamma_i$  for Xe<sup>+</sup> (Table I), we conclude that the reason for the  $\gamma_i$  change from tungsten to molybdenum is most likely the reduction in work function. Quantitative calculation of the effect has not been attempted. This would perhaps be appropriate after several atomically clean metals have been studied. The effect of change in the state density function in the metal (item 3 above) may be judged from some results published in the paper on theory.<sup>4</sup> Rather sizable changes in  $\gamma_i$  for the heavier

noble gases could be effected in changing from a constant state density function to a parabolic one (Table IV of reference 4). However, no such drastic change in the state density between molybdenum and tungsten is expected, and hence no great change in  $\gamma_i$  is attributable to this cause.

## VII. RESULTS FOR DOUBLY-CHARGED IONS

Measurements of electron yield,  $\gamma_{i2}$ , and energy distribution for electrons ejected from molybdenum by doubly-charged ions of the noble gases are shown in Figs. 11 and 12, respectively. The quality of the distribution function data may be judged from Fig. 13 which shows the  $\Delta\rho/\Delta V_{ST}$  step function curve and points from the smoothing curve as discussed in connection with Fig. 4. Bombarding electron energy in the ion source was 100 eV. The data of Figs. 11 and 12 were more carefully taken than the corresponding data for tungsten. Data for  $\gamma_{i2}$  were taken at smaller intervals of  $V_{ST}$ .

We turn now to a discussion of the processes in which a doubly-charged ion is neutralized and de-excited at an atomically clean metal surface. Because of the high probability of electron tunneling between metal and ion, it appears very likely that the doubly-charged ion is first partially neutralized to an excited state of the singly-charged ion. The electronic transition is of the type indicated between the energy levels  $a$  and  $b$  in Fig. 14. This partial resonance neutralization of the doubly-charged ion has been discussed to some extent elsewhere<sup>5</sup> in connection with estimation of the electron yield for the metastable singly-charged ion. Both theory and experiment concerned with resonance and Auger-type transitions between a metal and a normal singly-charged ion indicate that the resonance process is much more probable than the Auger process at a given distance from the surface. Thus the resonance process occurs before any Auger process as the ion approaches the metal surface.

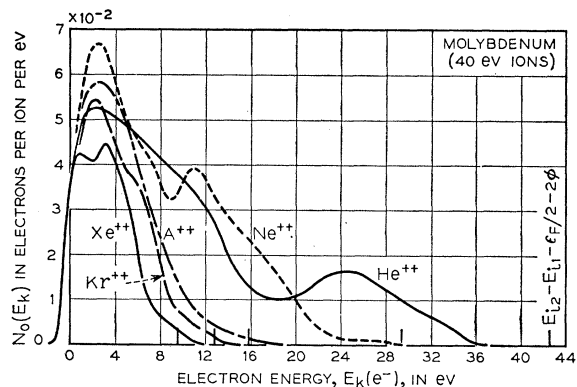


FIG. 12. Energy distributions of electrons ejected from molybdenum by doubly-charged ions of 40-eV kinetic energy. The vertical lines along the energy axis indicate the values of  $E_{i2} - E_{i1} - (\epsilon_F/2) - 2\varphi$  as discussed in the text.

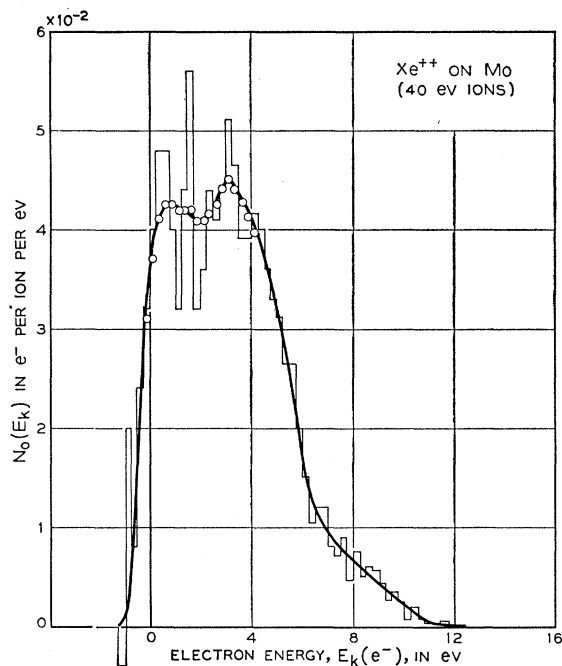


FIG. 13. Data typical of that upon which the energy distributions of Fig. 12 are based. The step curve is the  $\Delta\rho$  vs  $\Delta V_{ST}$  curve obtained directly from the original data. The points are calculated from a smoothing formula which employs eight adjacent data points and the full curve is taken to represent the true distribution. It is the curve plotted for  $\text{Xe}^{++}$  in Fig. 12.

The excited (possibly metastable) singly-charged ion formed near the metal surface by resonance tunneling may decay to the ground state of the normal parent atom in more than one conceivable manner. It is convenient in this discussion to consider the energy levels for the normal, singly-charged, and doubly-charged ions of argon, krypton, and xenon shown in Fig. 15. If we look at Fig. 15 we see that the excited singly-charged ion, whose energy is at or near one of the metastable levels, could conceivably reach the ground state of the normal atom either directly or in two or more steps involving transitions to the ground state of the ion or excited states of the neutralized atom. However, we are led by the following series of arguments to the rather firm conclusion that the excited singly-charged ion is de-excited in two successive Auger-type processes.

1. The de-excitation and neutralization of the excited ion to the ground state of the parent atom must proceed in one or more Auger-type processes. The only other possibility, that of radiation of the energy released, is highly improbable on the grounds that radiation at its fastest requires about  $10^{-8}$  sec to proceed whereas the ion here spends a time of the order of  $10^{-11}$  to  $10^{-12}$  second within a few angstrom units of the metal surface.

2. The de-excitation and neutralization does not take place in one step. If such were the case and if only two electrons per ion were involved (one to neutralize, the second to be excited inside the metal), we should expect

to see much faster electrons outside the metal than are in fact observed. The maximum kinetic energy should then be of the order of  $E_{xi} + E_{i1} - 2\phi$  where  $E_{xi}$  is the excitation energy of the ion,  $E_{i1}$  the first ionization energy, and  $\phi$  the work function of the target. Instead, the maximum kinetic energy is more nearly equal to  $E_{xi} - \phi$ , the value to be expected if the process giving rise to the fastest electrons involves only de-excitation of the ion to its ground state. If the electron which tunnels through from the metal to neutralize one charge of the doubly-charged ion does so on the average at the middle of the band, then  $E_{xi} = E_{i2} - E_{i1} - (\phi + \epsilon_{F/2})$ . Then the maximum kinetic energy is  $E_{i2} - E_{i1} - (\epsilon_{F/2}) - 2\phi$ , which is indicated for each ion on the energy axis in Fig. 12.

De-excitation and neutralization in a single process involving more than two electrons could yield an  $N_0$  function in agreement with that observed since the available energy would then be shared by two or more excited electrons. Such processes would be expected to be much less probable than that involving a total of only two electrons. It appears not to be necessary to postulate the involvement of more than two electrons to explain any of the observations concerning any kind of atomic Auger process.<sup>21</sup> Since the single process

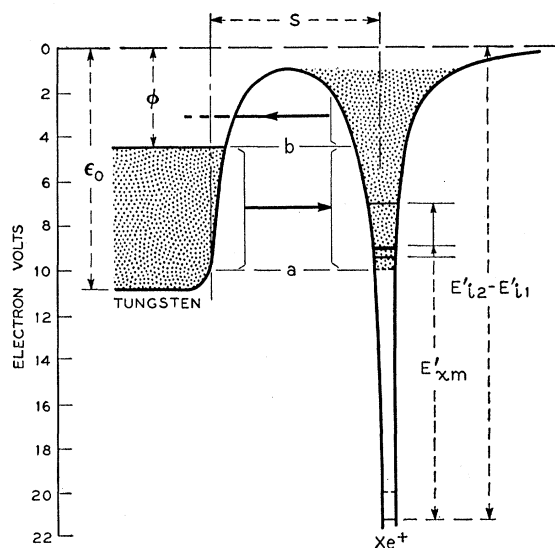


FIG. 14. Energy level diagram indicating the resonance tunneling transitions which can occur from tungsten into the doubly-charged xenon ion or from the excited singly-charged xenon ion into the metal. Energy of a test electron is plotted vertically. The metal is to the left. The atomic particle is to the right at a distance  $s$  from the metal surface. The filled portion of the conduction band in tungsten is shown stippled. Energy levels in the atomic particle are those of an electron moving in the field of the singly-charged core. Lowest lying excited states are indicated as dashed lines, metastable levels as full lines, and by stippling is indicated the region of relatively large density of excited levels. Tunneling into the ion can occur between levels  $a$  and  $b$ , from the ion into the metal above  $b$ .

<sup>21</sup> E. H. S. Burhop, *The Auger Effect and Other Radiationless Transitions* (Cambridge University Press, New York, 1952).

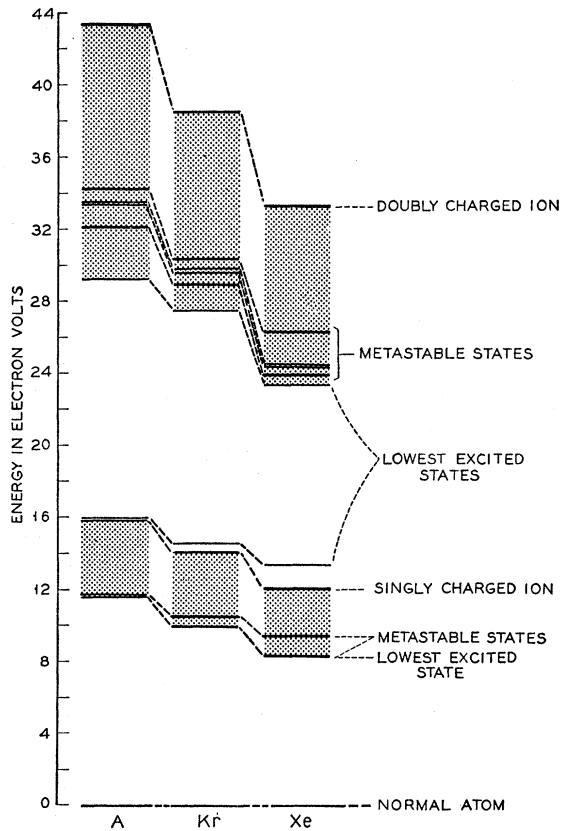
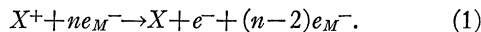


FIG. 15. Energy levels in argon, krypton, and xenon. Lowest excited levels and metastable levels are indicated individually. Regions where other excited levels are to be found are stippled.

involving two electrons does not occur, we conclude that the process proceeds in two or more stages.

3. The process in all probability proceeds in only two steps. First we see that the last stage must be Auger neutralization of the normal ion:

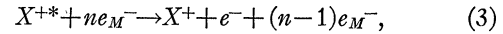


In this equation  $X$  represents the normal atom,  $X^+$  the ion,  $e_M^-$  an electron in the metal,  $e^-$  a free electron, and  $n$  the number of electrons originally in the metal. We note in Fig. 15 that the only intermediate states between the excited ion  $X^{+*}$  and  $X$  in each case,  $X = A, Kr, \text{ or } Xe$ , are the ground state of the singly-charged ion and the excited states of the atom lying just below them. We are justified in neglecting the presence of the excited state of the ion which lies just above the ground state because its involvement rather than the ground state could not be detected in any way in these experiments. Should the result of all previous stages but the last conceivably result in an excited atom, this atom should be ionized directly by the process of resonance ionization:

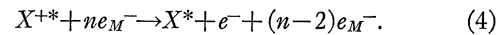


Finally, because of the large gap between the ground

state of the ion and its excited states only one detectable first stage is possible and must be either an Auger-type de-excitation to the normal ion:



or a conceivable Auger-type neutralization to an excited state of the atom:



If process (4) occurred, it would, as we have indicated, be followed immediately, certainly for  $X = He, A, Kr, \text{ or } Xe$ , by resonance ionization (2) of the excited atom. From the point of view of quantum mechanics this means that an electron in the system of atom and metal in close proximity could not exist in the atom at the energy levels of the excited state. The wave functions at these energies lie essentially entirely within the metal. In this sense there is really no final state  $X^*$  for process (4) when the atom is near the metal. We conclude that process (4) as such cannot occur. Thus the de-excitation and neutralization of the excited ion for He, A, Kr, and Xe involves process (3) above followed by process (1). This should also be true for Ne except for the possibility that, when the particle is farther from the metal than the so-called critical distance,<sup>4</sup> process (2) will not occur because the excited state

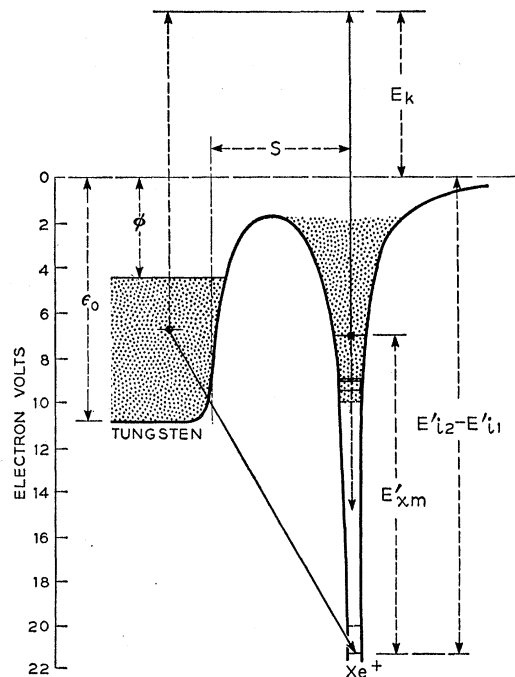


FIG. 16. Energy level diagram indicating the electronic transitions which occur in the process of Auger de-excitation of an excited ion of xenon at a tungsten surface. Transitions involving electron exchange between metal and ion are indicated by full lines, those not involving electron exchange by dashed lines. This is the second stage of the process by which a doubly-charged ion moves to the ground state of the parent atom at a metal surface.

$\text{Ne}^m$  lies below the top of the conduction band. Then process (4) is possible for Ne. If, however, these processes occur closer to the surface than the critical distance, process (2) will occur and Ne will behave like the other noble gases.

We conclude that the neutralization and de-excitation of a doubly-charged ion at an atomically clean metal surface involves:

1. Resonance neutralization to an excited state of the singly-charged ion. (Fig. 14.)
2. Auger de-excitation of the excited singly-charged ion to the ground state of the ion. [Process (3); Fig. 16.]
3. Auger neutralization of the singly-charged ion to the ground state of the atom. [Process (1); Fig. 17.]

These stages follow one another in order as the atomic particle approaches the metal surface. Electrons are ejected from the metal in the second and third of these stages. In the third stage the number of electrons ejected per ion should be approximately  $\gamma_i$  and thus in the second stage approximately  $\gamma_{i2} - \gamma_i$  electrons are ejected per ion. It is seen from Table I that  $\gamma_{i2} - \gamma_i$  is much larger than  $\gamma_i$ . It has been possible to calculate a value for  $\gamma_{i2} - \gamma_i$  for xenon by the methods of the theory published in reference 4. This gives for xenon and molybdenum  $\gamma_{i2} - \gamma_i = 0.22$  whereas the experimental value is 0.23. This agreement is really too good because the excited state of the singly-charged ion  $\text{Xe}^{+*}$ , was taken for the purposes of this calculation to be the lowest metastable level, a level which might well be somewhat too low on the average. Furthermore, one cannot say that the yield for the third stage is exactly equal to  $\gamma_i$  as measured for a singly-charged ion for the following reason. When one sends the singly-charged ion toward the surface Auger neutralization will occur as a function of distance of the ion from the surface in a different way from that which occurs when this process is the third stage of a series of processes oc-

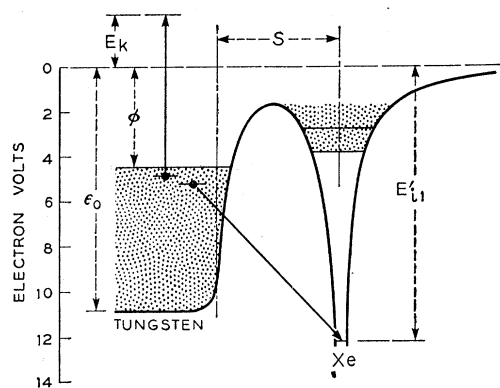


FIG. 17. Energy level diagram indicating the electronic transitions which occur when the normal singly-charged ion of xenon is neutralized in the process of Auger neutralization. This is the third stage of the process by which a doubly-charged ion reaches the ground state of the parent atom.

ccurring as the atomic particle approaches the surface. One might expect the third stage to occur closer to the metal than does the Auger neutralization of the singly-charged ion which approaches from infinite distance as such. This would tend to reduce the yield from the third stage below the measured  $\gamma_i$  for a singly-charged ion because of the reduction of effective ionization energy as the distance between metal and particle decreases.

Although there are metastable excited states of  $\text{Xe}^{++}$ ,  $\gamma_{i2}$  for xenon was found to be independent of bombarding electron energy in the ion source above  $E_{i1}$ . Thus the cross section for formation of metastable doubly-charged ions is so low as to be undetectable in xenon and presumably in the other noble gases as well.

The author wishes to acknowledge with thanks the technical assistance of C. D'Amico who recorded all of the experimental data on which this work is based. He wishes also to thank D. J. Rose for critical reading of the manuscript.